Title: Evaluating the effect of biochar addition on the anaerobic digestion of swine manure: Application of Py-GC/MS

Authors: Xiomar Gómez[a*], William Meredith[b], Camino Fernández[a], Mario Sánchez-García[c], Rebeca Díez-Antolínez[a], Jorge Garzón-Santos[c], Collin E. Snape[b].

Affiliations:

[a] Chemical and Environmental Bioprocess Engineering Department, Natural Resources Institute (IRENA), University of León, Avda. de Portugal 41, 24071, León, Spain.

[b] Faculty of Engineering, University of Nottingham, The Energy Technologies Building, Innovation Park, Jubilee Campus, Triumph Road, Nottingham, NG7 2TU, UK.

[c] Research Institute of Vine and Wine (IIVV), University of León, Avda. de Portugal 41, 24071, León, Spain.

[*] Corresponding author:

E-mail address: xagomb@unileon.es

This is a pre-print of an article published in Environmental Science and Pollution Research. The final authenticated version is available online at:

https://link.springer.com/article/10.1007/s11356-018-2644-4

Cite as:

Gómez, X., Meredith, W., Fernández, C. et al. Environ Sci Pollut Res (2018). https://doi.org/10.1007/s11356-018-2644-4.

Abstract

The anaerobic digestion process of swine manure was studied when char was used as supplement for improving performance. The use of pyrolysis-gas chromatography/mass spectrometry (Py-GC/MS) was proposed for assessing the organic matter degradation. The assessment on biogas production was carried out using samples of swine manure (SM) supplemented with char in one case and pre-treated by microwave irradiation in the other. This experimental set-up allows for the comparison of the biological degradation observed under these two different configurations and therefore aids in understanding the effect of char particles on the process. Results showed similar performance for both systems, with an average improvement of 39% being obtained in methane production when compared to the single digestion of SM. The analysis of digestate samples by Fourier Transform Infrared (FTIR) Spectroscopy and Py-GC/MS showed improved degradation of proteins, with the Py-GC/MS technique also capable of identifying an increase in microbial derived material when char was added; therefore highlighting the relevant role of carbon conductive particles on biological systems. Py-GC/MS along with the use of (FTIR) Spectroscopy has proven to be useful tools when evaluating anaerobic digestion.

Keywords: *Biochar, PY-GC/MS, FTIR, microwave pre-treatment, anaerobic digestion*

Introduction

The potential use of carbon-based conductive materials in anaerobic digestion processes has gained great interest in recent years due to a great variety of reports claiming the benefits associated with the increase in methane yields and attenuation of inhibitory effects (Cai et al. 2016; Cuetos et al. 2016). Biochar (obtained from the thermochemical conversion of biomass) and its use in land application has been traditionally proposed as a means for increasing the carbon storage capacity of soils, enhancing their properties and influencing the soil bacterial community (Wang et al. 2015) and a suitable soil amendment for minimising the negative effects of heavy metals on soils (Gusiatin et al. 2016). In recent years, the addition of biochar to digestion systems has proven to be a good alternative for providing new synergies between two traditional processes, as it is the pyrolysis of lignocellulosic biomass and the digestion of wastes (Song et al. 2017). In addition, the use of microalgae chars (Kim et al. 2016) and lignocellulosic biomass offers a good prospect to escape from the dilemma of biofuel versus food production (Roth and Spiess 2015).

Recent approaches for increasing the economic feasibility of waste treatment processes involve the conjunction of thermal and biological treatments in an attempt to increase energy efficiency and reduce the volume of side streams which can find limited disposal options. Swine manure is an organic stream that presents a high energy-production potential (Han et al. 2018). However, the use of complex substrates has been associated with inefficiencies in the digestion process due to the slow rate of the first hydrolysis stage. In an attempt to increase biogas yield and improve the degradation of organic materials, the application of different pre-treatments have been studied (e.g. thermal,

alkaline, acid, chemical, mechanical, etc.) (Feki et al. 2015; Donoso-Bravo et al. 2016; Martínez et al. 2017), although in some cases, their large scale implementation may be limited due to their low economic feasibility.

On the other hand, the combination of anaerobic digestion and pyrolysis allows for new synergies, which results in improvements thanks to the addition of biochar to the reactor liquor. Recent studies on the performance of anaerobic digestion supplemented with char report on the enhancement of the process by avoiding inhibitory conditions or promoting the growth of methanogens (Luo et al. 2015; De Vrieze et al. 2016). Direct interspecies electrons transfer (DIET) has also been suggested as one of the reasons for obtaining better degradation rates when carbon-based conductive materials are added (Dang et al. 2016). Although, several reports can be found in literature about the effects of adding conductive carbon materials to biological systems, there is still missing information about the evolution of the organic matter during biological transformations, and to what extent the improvement obtained with the addition of conductive materials may be comparable to those obtained from the application of different pre-treatment technologies.

Pyrolysis-gas chromatography/mass spectrometry (Py-GC/MS) has been widely applied for the study of complex materials such as soil organic matter and recently for biomass characterisation (Liu et al. 2016; Zhu et al. 2016). The main advantages of the pyrolysis route for analysing complex organic samples are minimal sample preparation, minimum time of analysis and relative low cost (Prasad et al. 2006). There exists a wide experience in the application of spectroscopic techniques for evaluating the transformation of the organic material by biological process such as composting, soil

organic matter degradation and anaerobic digestion (Mopper et al. 2007; Kataki et al. 2017) allowing to elucidate the main relevant factors involved. In the present research the use of Py-GC/MS, along with spectroscopy techniques as it is Fourier Transform Infrared (FTIR) Spectroscopy has been investigated as tools for evaluating the effects of biochar addition on anaerobic digestion systems.

The aim of this experimental work was the assessment of the anaerobic digestion of swine manure (SM) following biochar addition as a means for improving system performance. A comparison of performance is carried out to evaluate the effect of supplementing the process with biochar particles. The process was evaluated using as substrates SM and pre-treated SM by microwave irradiation. The pre-treated system was used as reference for evaluating the modifications attained during digestion. Py-GC/MS and FTIR were used for evaluating the biological performance.

Materials and methods

Substrates and inoculum

SM was collected from a livestock farm located in the surroundings of the City of León (Spain). The manure was stored at 4 ºC until required for use. The anaerobic sludge used as inoculum was obtained from the wastewater treatment plant of León where the anaerobic digester operates under mesophilic conditions (32 – 34 ºC at an average hydraulic retention time of 30 d). The digested sludge obtained from the wastewater treatment plant was stored in closed vessel with a biogas release device and at room

123 temperature conditions (22 ºC) for a month. This was done to allow the release of
124 biogas and avoid interferences during the batch experiments.
125
126 The chemical characteristics of SM and inoculum are presented in Table 1. Char was
127 produced from residual biomass of almond shell provided by "BIOTERM
128 AGROFORESTAL SL" (Córdoba, Spain). Raw biomass and char samples were
129 characterised as described by Alburquerque et al. (2016). Almond shells had volatile
130 matter (VM) content of 821.4 g/kg and an ash content of 5.5 g/kg. The char was
131 produced in a semi-continuous electrically heated reactor at 550 ºC. The char thus
132 produced had a VM content of 88.6 g/kg and an ash content of 31.2 g/kg. Further details
133 of the operating conditions and char chemical and physical characteristics are described
134 by Gómez et al. (2016). The mean particle size was 225 µm for the biochar fraction
135 used for digestion experiments.
136
137 Table 1
138
139 **Batch digestion experiments**
140
141 Digestion experiments were performed using SM and microwave pre-treated SM as the
142 substrate. Batch digestion tests were carried out in Erlenmeyer flasks with a working
143 volume of 250 mL. Flasks were stirred at 125 rpm and maintained at 35 ± 1 ºC by
144 means of a water bath. Each reactor contained 1.5 g of volatile solids (VS) from
145 manure. Inoculum was added to attain a VS ratio of 1.0 —inoculum-substrate (I/S)—.
146 Water was added to complete the 250 mL volume. Four reactors were used in each
147 experiment. Two replicates were used for measuring biogas production and

148 composition, while the other two were used for monitoring the liquid phase. A control
149 assay was also run in parallel to measure the background gas production from the
150 inoculum. Reactors were denoted as SM for the one digesting this substrate and
151 SM_MW for the one treating microwave pre-treated SM.
152
153 Char was added to a set of batch digestion experiments to evaluate the effect on gas
154 production and organic matter degradation. 3.0 g of char (dry basis) were added to each
155 batch reactors. The experimental conditions were kept the same way as described above
156 but with the addition of char in this latter case. Therefore, these reactors were denoted
157 as SM_Char and SM_MW_Char.
158
159 Gas and liquid samples were taken twice a week to measure the composition of biogas
160 and the concentration of volatile fatty acids (VFAs). Gas production was measured daily
161 using a liquid displacement bottles filled with an acid and high salinity solution to avoid
162 CO_2 absorption. The gas stored by these devices was sampled using gas syringe and
163 composition was measured by gas chromatography as described in analytical techniques
164 section. The duration of the experiments was based on the observation of total stoppage
165 of gas production.
166
167 Curves of specific methane production were fitted to a modified Gompertz equation (1).
168 This model has been successfully tested for adjusting biogas data obtained from batch
169 digestion assays (Cuetos et al. 2013):
170

171 $$P_{(t)} = P_{\max}.\exp\left[-\exp\left[\frac{R_{\max}.e}{P_{\max}}(\lambda - t)+1 \right] \right] \quad (1)$$

172

Where *P(t)* is the cumulative values of the specific methane production (mL/kg VS), *Pmax* is the maximum value obtained for the specific methane production (mL/kg VS), *Rmax* is the maximum production rate (mL/kg VS d), λ is the lag-phase time (d) and *e* is 2.71. The software OriginPro was used for fitting data to the equation and obtaining the model parameters *Pmax*, *Rmax*, and λ.

Microwave pre-treatment

SM was pre-treated using a 1500 W/2455 MHz microwave oven MARS (CEM, North Carolina, USA). The pre-treatment assay was performed by fixing power at 600 W (maximum efficiency 80%). The temperature was increased with a ramp of 10 ºC/min until reach 80 ºC and hold during 15 min. Temperature was controlled by an Infrared (IR) temperature probe. The fresh SM was pre-treated by microwave (solid content of 23.1 g/L, see Table 1). 500 g of this substrate were pre-treated by equally distributing the sample in 10 rotating vessels on the carousel.

Analytical techniques

Kjeldahl nitrogen (KN), total solid (TS), VS, alkalinity, ammonium, and pH were measured in accordance with American Public Health Association (APHA) standard methods (2012). Total phosphorous (TP) was measured by the use of inductively coupled plasma atomic emission spectrometer (ICP-AES) (Perkin Elmer Optima 2000 DV). Gas production data were normalised to standard temperature and pressure (0 ºC and 1 atm). Biogas composition and VFAs were analysed using a gas chromatograph (Varian CP 3800 GC) as described by Martínez et al. (2017).

Proximate analysis was performed according to ASTM 3302 for total moisture, UNE 3219 for analysing volatile matter and UNE 32004 for ash analysis. Proximate analyses of the oven dried samples were carried out using a LECO MAC-300 thermogravimetric analyzer (TGA). A LECO CHN-600 apparatus was used for the analysis of C, H and N according to ASTM 5373. Sulphur was measured on a LECO SC-132, according to ASTM 4239. The O content was calculated by difference of the sum of C, H, N, and S values from 100% (on a dry ash-free basis). Biochar particle size analysis was performed using a Laser Diffraction particle Size Analyser LS 13 320 Beckmann Coulter. Samples selected for analysis were those comprising the initial state of the experiment (SM and inoculum) and those obtained from the final stage of the batch digestion test (digestates from the different experimental sets).

The surface of solid samples obtained after dismantling of reactors was analysed by scanning electron microscopy (SEM). Char and digestate samples were obtained after sedimentation of the reactor liquor and drying at 105 ºC. Samples were ground using an agate mortar. Samples were sputter-coated with gold in high vacuum (0.05 – 0.07 mbar) with a coater Blazers SCD 004. The samples were examined using a JEOL JSM 6840 LV scanning electron microscope.

Infrared spectra of substrate and digested samples were recorded using an FTIR Thermo Scientific Nicolet iS5 (ID7 ATR accessory, a monolithic diamond ATR crystal with high-efficiency) spectrophotometer over the 4000 – 650 cm^{-1} range at a rate of 0.5 cm/s. Sixteen scans were collected with 0.482 cm^{-1} spacing, averaged for each spectrum and corrected against ambient air as background.

223

224 **Py-GC/MS**

225

226 Py-GC/MS analysis was conducted using a CDS Analytical 5200 pyroprobe, coupled
227 with an Agilent GC-MS (7890B GC; 5977A MSD). The probe has a temperature range
228 of 1–1400 ºC, and a heating rate up to 20 ºC/ms. A sample of homogeneous powder
229 (approximately 5 mg) was placed in a quartz capillary tube (length 25 mm; diameter 2
230 mm) and secured at each end with quartz wool. Pyrolysis was carried out to a final
231 temperature of 700 ºC, with a heating rate of 20 ºC/s and the final temperature then held
232 for 60 s. Products were retained on a Tenex trap before desorption at 280 ºC (for 4 min)
233 and passage to the GC via a heated transfer line (310 ºC). Product separation was
234 performed on an HP-5MS column (30 m x 250 μm x 0.25 μm). The GC oven
235 temperature was initially held at 50 ºC for 0.5 min, then heated to 300 ºC at a rate of 4
236 ºC/min, where it was held for 5 min. The MS (EI of 70 eV) scanned in the mass range
237 of m/z 40 – 400, with an ion source temperature of 200 ºC. Individual compounds were
238 identified using a NIST MS library and published data.

239

240 Two multivariate statistical methods, Hierarchical Cluster Analysis (HCA) and
241 Principal Component Analysis (PCA), were used for the evaluation of the samples
242 based chromatograms obtained form Py-GC/MS. HCA was used to classify the studied
243 samples into different groups. Grouping in clusters was carried out using Ward's
244 algorithm. Results are presented in the form of dendrograms.

245

246 PCA can be applied by creating a discrete data set of signals and representing these as
247 linear combinations of a set of factors. The major advantage of this statistical method is

its ability to reduce the dimensionality of the data set by eliminating redundant dimensions and identifying meaningful underlying variables that better represent the differences and similarities in a specific data set (Abdulla et al. 2013). Usually, only the first few principal components in a descending order explain the maximum of the total variance of all original variables. The score plot of the first principal components was used to investigate the inter-relationships between the samples, as it allowed the observation of clusters of samples (Martínez et al. 2016). Both HCA and PCA were performed using OriginPro software.

3. Results and discussion

3.1. Digestion experiments

Results from proximate and ultimate analysis are shown in Table 2. The inoculum sample presents high ash content associated with the degree of mineralisation of this sample. The digested sludge presented a low volatile content. This sludge was previously stored at room temperature to avoid interferences with the biogas production of the samples during the batch experiments. During this storage period, microbial activity led to the reduction in volatiles and readily degradable material resulting in a decrease in total solid content and enrichment in complex compounds and minerals.

Table 2

Digestate obtained from the experiment treating SM as sole substrate, presented also a marked increase in the ash content. This is explained by the high value of the substrate,

with an ash content of 27.2%. The mixture of this material with the inoculum which was also characterised by high inorganic concentration leads to an initial ash content of 33.6%. Starting the digestion with such high mineral content results in a digestate with remarkably high mineral components. The increase in ash content was of 38.8%, which was also similar to the cases of the pre-treated SM batch experiment.

The pre-treatment of the substrate by microwave (MW) irradiation did not have any effect on results obtained from proximate analysis, with similar values in volatiles and ash content being reported. The addition of char to the mixture highly affected results from proximate and ultimate analysis due to the high organic carbon content of this material, but no effect was observed on elements measured.

Differences in methane production and its rate can be observed in Fig. 1a. The digestion of SM was characterised by a delay in biogas production (See λ value in Table 3) probably caused by the change in environmental conditions. Previous to the experiments, the inoculum was stored at room temperature conditions for a month period without any kind of substrate being supplied. The change from the storage to the conditions of the experiments may explain the delay observed in the production of biogas for all assays studied. In addition, the ammonium content of this inoculum was much lower than that of the substrate (Table 1); therefore the initial value of the batch reactors was in the range of 1300 to 1400 mg/L (See Fig. 1b). This change in ammonium concentration and the high mineralisation of the inoculum used may be the main reason for explaining the null biogas production during the initial stage.

Fig. 1

298

299 Table 3

300

301 The addition of char resulted in a decrease in the lag phase and also affected in a
302 positive way the methane production rate and the final cumulative value. Positive
303 effects have also been observed by different authors when evaluating the use of char and
304 conductive carbon materials in anaerobic digestion (Liu et al. 2012; Cuetos et al. 2016;
305 Dang et al. 2016). The aggregation of cells is considered a key factor for efficient
306 methanisation as a direct result of better electron transfer between obligate H_2-
307 producing acetogens and methanogens. Direct interspecies electrons transfer (DIET) is a
308 syntrophic metabolism in which free electrons flow from one cell to another without
309 being shuttled by reduced molecules such as molecular hydrogen or formate (Dubé and
310 Guiot 2015). It is believed that an improvement in this mechanism by the presence of
311 conductive materials directly results in higher gas yields. It is considered that the
312 presence of conductive carbon materials allows for an effective connection between
313 cells that are not strictly in physical contact with each other. It is suggested that electron
314 transport carriers associated with the outer surface of the cell are able to make the
315 required electrical contacts with the conductive material (Chen et al., 2014; Lovley
316 2017) resulting in an enhancement of methane production (Wang et al., 2017)

317

318 The irradiation of the substrate by MW resulted in the loss of ammonium. The pre-
319 treated sample of SM presented an ammonium concentration of 2775 mg/L which
320 resulted in slightly lower values of ammonium content for batch reactors using this
321 substrate (see Fig. 1b). This change may not seem relevant enough to be considered as
322 the responsible for the difference observed in the lag phase values. The addition of char

and the application of a pre-treatment may have facilitated the degradation of the organic material by the anaerobic microflora causing as a result a reduction in the initial lag-phase observed for these systems. The final ammonium concentration measured at the end of the digestion tests present similar values for the four assays evaluated (see Table 3).

MW irradiation also exerted a positive effect on methane production. Digestion systems fed with the pre-treated substrate showed higher methane content in biogas probably as a result of a better degradation of nitrogen containing material. Higher release of ammonium is observed in Fig. 1b for pre-treated systems, although at the end of the digestion these reactors presented lower ammonium content which may be explained by the loss of this compound by volatilisation. However, the addition of char in experiments using pre-treated SM did not report additional significant changes in the performance of the digestion process. Methane curves obtained from these experiments presented a quite similar gas evolution profile to those from the pre-treated system without biochar.

The pre-treatment may have facilitated the degradation of complex material like proteins and the lipid fraction of the SM. This effect is observed by the slope of the cumulative methane production curve, which represents the methane production rate. SM digestion systems present a change in the slope of the curve associated with the complexity of the material being degraded. Right after the lag phase, the slope of the curve obtained for the SM digestion system was 25 mL CH_4/kg VS d (days 10–19) and this value was reduced to 6.4 mL CH_4/kg VS d on the following stage (days 21–39). The SM_Char system presented a similar behaviour, but with higher rates being

obtained in each stage (29.4 and 9.0 mL CH_4/kg VS d for the two different stages). The application of MW irradiation resulted in a homogenous degradation profile, where differences in the methane production rate were eliminated once the lag phase had elapsed. The improvement of MW pre-treatment on anaerobic digestion has been demonstrated by several authors (Tyagi et al. 2014; Yeneneh et al. 2017). Changes experienced by the organic material and modifications in the specific surface area of the organic particles have been proposed as the reasons given for obtaining an enhancement in digestion when MW pre-treatment is applied (Martínez et al. 2017). In the present study the methane yield from pre-treated systems and biochar aided systems was about 420 mL CH_4/g VS, while in the SM reactor this value was 28% lower.

The addition of char did not represent any significant changes in the evolution of NH_4^+ content in the different experiments. Values of this parameter were quite similar for the different experiments indicating that the adsorption of this cation on the char surface can be disregarded as the cause for improving the performance of the digestion process when SM was treated.

Fig. 1 also presents the evolution of VFA in batch tests. The anaerobic degradation of SM was characterised by high VFA production (Fig. 1c). These high values along with the negative effects associated with the ammonium levels in the reactor may have been responsible for the delay observed at the initial stage of the trial. Ammonium content in the reactor was below the threshold value considered as inhibitory (3.0 - 3.7 g/L for ammonium values and 1.0 -1.1 g/L for free ammonia values (Gallert and Winter 1997; Moestedt et al. 2016)). However, the ammonium concentration may have been high enough to affect the performance of the microflora since the anaerobic consortium had

not been previously adapted to this type of substrate and was stored at room temperature to avoid interference with the background biogas production.

Acetic acid reached values around 3 500 mg/L at the initial stage of the fermentation, indicating that the acidification stage and the subsequent consumption of this acid may be suffering imbalances. The addition of char did not change this trend, but the carbon particles may have offered a protective site to the anaerobic microflora explaining therefore the lower values of λ obtained for the SM_Char system. On the other hand, the application of the MW pre-treatment favoured the consumption of this acid due to the volatilisation of ammonium experienced by the substrate, lowering its level in the reactor and therefore enhancing the performance of acetotrophic methanoges. Acetic acid concentration in pre-treated reactors was below 1 500 mg/L. Values of λ were similar for both systems and were close to that derived from the SM_Char system, corroborating the hypothesis of available protective sites for anaerobic microflora.

Scanning electron microscopy

Images of the char surface and dried digestate particles are shown in Fig. 2, with the porous structure of char being easily observed. Digestate material, obtained from the SM batch digestion experiment, presents an irregular surface which is very different from the surface observed from the solid particles obtained from the experiment of SM digestion supplemented with char. The surface of particles presents a more corrugated structure with the porous associated to the char particles being observed at the centre of the photograph. Digestate solid particles seem to be fully covering the carbon conductive material. Surface analysis performed by the same microscope, reported a

carbon content of 87.1 ± 1.1% for the char particles, this value was just 41.7 ± 1.7% for the SM digestate and was increased to 65.9 ± 1.6% as a result of the presence of char in the sample.

Fig. 2

Results from FTIR analysis

The degradation of the organic material was studied by means of FTIR spectroscopy. Assignment of main absorption bands was based on Cuetos et al. (2009) and Fierro et al. (2016). Initial samples and digestates were evaluated. Fig. 3 shows the different spectra obtained.

Fig. 3

The spectrum of inoculum and substrate shows similar bands with the latter presenting higher intensities in some particular regions. A broad absorption band at 2 500–3 800 cm^{-1} is attributed to O–H vibration and it was common to all samples analysed, with the exception made for the sample of char. The peak centred at 3 400 cm^{-1} is ascribed to hydrogen vibrations of the OH groups of alcohols, phenols and organic acids, but also to amide hydrogen vibrations. The presence of aliphatic compounds is observed in the range 2 800–3 000 cm^{-1}, along with the signals at 1 450–1 410 cm^{-1} associated this latter with the CH_2 scissor deformation vibration. The SM sample presents a higher intensity band in this region which is significantly reduced after the anaerobic treatment (see spectra from digested samples). The protein region associated with nitrogen containing

compounds (absorption bands at about 1 650 and 1 540 cm^{-1}) also presents high intensity in this same sample while it was highly attenuated in the inoculum sample. This is also the case for the region at 1 300–1 230 cm^{-1}, which was ascribed to phospholipids (PO_2) asymmetric stretching, C–O in carboxylic acids and protein amide III band (C–H and N–H) (Provenzano et al 2015).

The inoculum sample also presents an important band at 1 630 cm^{-1} ascribed to aromatic structures, which also remains clearly identifiable in digestate samples. The high intensity band at 1 030 cm^{-1} was also recurrent in the different samples obtained from the digestion experiments and was also reported as characteristic of sludge and digestates (Fierro et al. 2016).

The degradation of SM under anaerobic conditions leads to the consumption of readily degradable organic matter, therefore the decrease in signals ascribed to aliphatic and carbohydrate regions are in consonance with this statement. The digestate samples present a relative increase of the aromatic signal (1 630 cm^{-1}) with regard to that of proteins at 1 550 cm^{-1}. In addition, the application of microwave pre-treatment allows for an improvement in the degradation of these compounds, an effect which was observed from the change in the relative intensity of the protein peak, with the SM_MW sample presenting a decrease in the intensity of this peak when compared to the one at 1 630 cm^{-1}. This effect was also observable when Char was added to the digestion process. However, the combination of pre-treatment and char addition did not lead to additional modifications in the organic matter. Digestate sample obtained in this latter case (char addition and MW pre-treatment), presented a similar FTIR spectra to that of

447 the char supplemented digestate. That is, with similar relative intensities when
448 comparing signals at 1 630, 1 550 and 1 410 cm^{-1}.
449
450 *3.4. Results from Py-GC/MS analysis*
451
452 Pyrograms represented in Fig. 4 show a wide diversity of peaks in SM_substrate sample
453 and inoculum. Clear differences are easily observable for some major peaks. The first
454 volatile compounds obtained present as main components butane and acetic acid (see
455 supplementary material SM1 and peak identification table in SM3). These short chain
456 compounds were reduced in digestate samples, with the exception of the SM_Char
457 digested sample which presents a relative intensity similar to that obtained for toluene.
458 Phenol derivatives can arise from the decomposition of proteins, polycarboxylic acids
459 (Bracewell et al. 1980) or polysaccharides (Wilson et al 1983). The different
460 performance in the digestion system when char was added to aid in the mineralisation of
461 the organic material is also observed in the Py-GC/MS profiles. The addition of char
462 allowed for a faster start-up of the batch digestion tests and aided in the degradation of
463 proteinaceous material as it was also observed in FTIR spectra. In the present case, this
464 behaviour is corroborated by the differences observed from the relative intensities of
465 toluene, C_2-benzene, styrene and phenol peaks with regard to those ascribed to short
466 chain molecules. The presence of toluene and styrene has been associated as a lignin
467 pyrolysis product; although styrene arises also very probably from non-hydrolysable
468 proteins, peptides and tannins (Dignac et al. 2006).
469
470 Fig. 4
471

Organic compounds of the furan type were identified among the pyrolysis products of the inoculum sample (furfural and 5-methyl furfural, see supplementary material SM1 and SM3), but were not discernible in the substrate sample neither in the digested samples. These compounds are considered as the pyrolysis products of polysaccharides (Dignac et al. 2005; El Fels et al. 2014) and furane type compounds have also been identified (furane and benzofurane) in the pyrolysis products of humic acids (Zhao et al. 2012) with their presence in the inoculum sample being probably associated with humic and fulvic substances.

Indole and methyl-indole were identified in the samples studied. These compounds have been recognised as pyrolysis products derived from tryptophan (Kebelmann et al. 2013). Other microbial pyrolysis products selected for tracking microbial signals, this case in sediments, are Benzyl nitrile, 2-furanmethanol, indole, phenol and pyrrole (Zhu et al. 2016). In the present study, phenol and Indole were clearly discernible in all chromatograms. Benzeneacetonitrile and benzenepropane nitrile can be also ascribed to microbial signals (See supplementary material).

Terrestrial lignocellulosic biomass yields a range of products such as acetic acid, furfural, syringol, vanillin, guaiacol, cresol, 2,3-dihydro-benzofuran, coniferyl alcohol and levoglucosan (Wu et al. 2010). Many of these compounds were also identified in the substrate and digestate samples, with particular incidence of cresol which presents a high intensity signal in the chromatograph of inoculum and digested samples.

SM_substrate and inoculum samples present a large amount of linear fatty acids as well as sterol components (Wang et al. 2015). Lipid fraction of sewage sludge and compost

has been analysed by different authors using NMR, pyrolysis–gas chromatography/mass spectrometry with tetramethylammonium hydroxide and spectroscopic techniques (Fierro et al. 2016; Li et al. 2017; Fukushima et al. 2018). In the present study C_{16} and C_{18} lipids and their fatty acid forms were identified in the substrate, inoculum and digested sample. These long chain compounds (oleic, stearic, and palmitic acids) have been described as major constituents of wastewaters (Palatsi et al. 2012).

Sterols presented a great contribution to the chromatogram obtained from the Py-GG/MS analysis of the inoculum sample. Among sterols, cholesterol is the main sterol of animal origin and in particular coprostanol which is used as marker of faeces (Volkman 1986). The recurrent appearance of sterols in digested samples is explained by the accumulation of these components during the digestion process. Due to their complex structure, these molecules were not affected by the microbial degradation.

Statistical analysis of Py-GC/MS chromatographs allowed the global evaluation of the samples. Results in Fig. 4 show a high correlation between the inoculum sample and the digested swine manure, irrespectively of the application of the MW pre-treatment. Although biogas evolution from the MW pre-treated sample represented an improvement in the biological degradation of the material which was observed by an increase in the biogas production rate (batch tests) and an improvement in the degradation of proteinaceous material (as observed in FTIR analysis), the digested material presents similar pyrolysis products to those obtained from the SM digestate sample, with the exception of the lipidic fraction which present signals with greater intensities in this latter case.

Statistical analysis also revealed that the presence of char is affecting the distribution of the pyrolysis products with those digestates containing char presenting a closer correlation. Py-GC/MS was capable of discerning differences in the evolution of the organic material when char was added to the digestion process. Pyrograms obtained from the char digestion systems present high intensity signals associated with the presence of microbial biomass and lignocellulosic compounds.

SM_substrate sample on the contrary, presented a great variety of compounds in the lipidic region (high contribution of -CH_2-) which were greatly reduced in all digested samples evaluated remaining only as major components of this region, those with C_{16} and C_{18} forms. The degradation of the organic content of SM by anaerobic digestion led to a great decrease of small molecules in pyrograms as evidence of the consumption by microorganisms of less complex compounds leading to the accumulation in digested samples of lignin type material and components derived from microbial biomass. Char addition accentuated the differences related to the distribution of organic compounds and this may be explained by the creation of a more favourable environment leading to an improvement in the development of microbial consortia as corroborated by different authors (Dang et al. 2016; De Vrieze et al. 2016).

4. Conclusions

This study of batch digestion systems of swine manure (SM) showed similar improvements in biogas yields for both the addition of biochar and microwave pre-treatment, demonstrating the great benefits of the addition of conductive carbon materials to biological processes. These results demonstrate the possibility of new synergies between traditional pyrolysis and digestion processes from a perspective of joining these two technologies in future biorefineries.

Py-GC/MS significantly aided in the interpretation of results regarding the transformation of organic components and was capable of discerning differences in the evolution of the different digestion tests by evaluating the distribution of pyrolysis products obtained from digested samples. A relative increase in microbial biomass pyrolysis products and lignin type material was observed for char containing samples while FTIR spectra although providing valuable information was limited in giving an explanation in the different performance when evaluating char supplemented systems and those of the microwave pre-treatment assay.

Acknowledgments

This research was possible thanks to the financial support of Project CTQ2015-68925-R and UNLE15-EE-3070 funded by Ministry of Economía y Competitividad, Spanish Government

Conflict of interests

Authors declare no conflict of interest

References

Abdulla HA, Minor EC, Dias RF, Hatcher PG (2013) Transformations of the chemical compositions of high molecular weight DOM along a salinity transect: using two dimensional correlation spectroscopy and principal component analysis approaches. Geochim Cosmochim Ac 118:231-246. https://doi.org/10.1016/j.gca.2013.03.036

Alburquerque JA, Sánchez ME, Mora M, Barrón V (2016) Slow pyrolysis of relevant biomasses in the Mediterranean basin. Part 2. Char characterisation for carbon sequestration and agricultural uses. J Clean Prod 120:191-197. https://doi.org/10.1016/j.jclepro.2014.10.080

A.P.H.A., Standard Methods for the Examination of Water and Wastewater, 22nd ed., American Public Health Association, Washington, DC, USA, 2012.

Bracewell JM, Robertson GW, Williams BL (1980) Pyrolysis-mass spectrometry studies of humification in a peat and a peaty podzol. J Anal Appl Pyrol 2:53-62. https://doi.org/10.1016/0165-2370(80)80045-3

Cai J, He P, Wang Y, Shao L, Lü F (2016) Effects and optimization of the use of biochar in anaerobic digestion of food wastes. Waste Manage Res 34:409-416. https://doi.org/10.1177/0734242X16634196

Chen S, Rotaru AE, Shrestha PM, Malvankar NS, Liu F, Fan W, Nevin KP, Lovley DR (2014) Promoting interspecies electron transfer with biochar. Sci Rep-UK 4:5019. doi:10.1038/srep05019

590 Cuetos MJ, Morán A, Otero M, Gómez X (2009) Anaerobic co-digestion of poultry
591 blood with OFMSW: FTIR and TG–DTG study of process stabilization. Environ
592 Technol 30:571-582. https://doi.org/10.1080/09593330902835730
593 Cuetos MJ, Gómez X, Martínez EJ, Fierro J, Otero M (2013) Feasibility of anaerobic
594 co-digestion of poultry blood with maize residues. Bioresource Technol 144:513-520.
595 https://doi.org/10.1016/j.biortech.2013.06.129
596 Cuetos MJ, Martínez EJ, Moreno R, González R, Otero M, Gómez X (2016) Enhancing
597 anaerobic digestion of poultry blood using activated carbon. J Adv Res 8:297-307.
598 https://doi.org/10.1016/j.jare.2016.12.004
599 Dang Y, Holmes DE, Zhao Z, Woodard TL, Zhang Y, Sun D, Lovley DR (2016)
600 Enhancing anaerobic digestion of complex organic waste with carbon-based conductive
601 materials. Bioresource Technol 220:516-522.
602 https://doi.org/10.1016/j.biortech.2016.08.114
603 De Vrieze J, Devooght A, Walraedt D, Boon N (2016) Enrichment of Methanosaetaceae
604 on carbon felt and biochar during anaerobic digestion of a potassium-rich molasses
605 stream. Appl Microbiol Biot 100:5177-5187. https://doi.org/10.1007/s00253-016-7503-
606 y
607 Dignac MF, Houot S, Francou C, Derenne S (2005) Pyrolytic study of compost and
608 waste organic matter. Org Geochem 36:1054-1071.
609 https://doi.org/10.1016/j.orggeochem.2005.02.007
610 Dignac MF, Houot S, Derenne S (2006) How the polarity of the separation column may
611 influence the characterization of compost organic matter by pyrolysis-GC/MS. J Anal
612 Appl Pyrol 75:128-139. https://doi.org/10.1016/j.jaap.2005.05.001
613 Donoso-Bravo A, Ortega-Martinez E, Ruiz-Filippi G (2016) Impact of milling, enzyme
614 addition, and steam explosion on the solid waste biomethanation of an olive oil

615 production plant. Bioproc Biosyst Eng 39:331-340. https://doi.org/10.1007/s00449-015-
616 1519-z
617 Dubé CD, Guiot SR (2015) Direct interspecies electron transfer in anaerobic digestion:
618 A Review. In: Guebitz GM, Bauer A, Bochmann G, Gronauer A, Weiss S (Eds.),
619 Biogas Science and Technology, Springer International Publishing, Switzerland, pp.
620 101–115
621 El Fels L, Lemee L, Ambles A, Hafidi M (2014) Identification and biotransformation of
622 lignin compounds during co-composting of sewage sludge-palm tree waste using
623 pyrolysis-GC/MS. Int Biodeter Biodegr 92:26-35.
624 https://doi.org/10.1016/j.ibiod.2014.04.001
625 Feki E, Khoufi S, Loukil S, Sayadi S (2015) Improvement of anaerobic digestion of
626 waste-activated sludge by using H2O2 oxidation, electrolysis, electro-oxidation and
627 thermo-alkaline pretreatments. Environ Sci Pollut R 22:14717-14726.
628 https://doi.org/10.1007/s11356-015-4677-2
629 Fierro J, Martinez EJ, Rosas JG, Fernández RA, López R, Gomez X (2016) Co-
630 digestion of swine manure and crude glycerine: increasing glycerine ratio results in
631 preferential degradation of labile compounds. Water Air Soil Poll 227:1-13.
632 https://doi.org/10.1007/s11270-016-2773-7
633 Fukushima M, Tu X, Aneksampant A, Tanaka A (2018) Analysis of branched-chain
634 fatty acids in humic substances as indices for compost maturity by pyrolysis–gas
635 chromatography/mass spectrometry with tetramethylammonium hydroxide (TMAH-py–
636 GC/MS). J Mater Cycles Waste 20:176-184. https://doi.org/10.1007/s10163-016-0559-z
637 Gallert C, Winter J (1997) Mesophilic and thermophilic anaerobic digestion of source-
638 sorted organic wastes: effect of ammonia on glucose degradation and methane
639 production. Appl Microbiol Biot 48:405-410. https://doi.org/10.1007/s002530051071

640 Gómez N, Rosas JG, Cara J, Martínez O, Alburquerque JA, Sánchez ME (2016) Slow
641 pyrolysis of relevant biomasses in the Mediterranean basin. Part 1. Effect of temperature
642 on process performance on a pilot scale. J Clean Prod 120:181-190.
643 https://doi.org/10.1016/j.jclepro.2014.10.082
644 Gusiatin ZM, Kurkowski R, Brym S, Wiśniewski D (2016) Properties of biochars from
645 conventional and alternative feedstocks and their suitability for metal immobilization in
646 industrial soil. Environ Sci Pollut R 23:21249-21261. https://doi.org/10.1007/s11356-
647 016-7335-4
648 Han G, Shin SG, Cho K, Lee J, Kim W, Hwang S (2018) Temporal variation in
649 bacterial and methanogenic communities of three full-scale anaerobic digesters treating
650 swine wastewater. Environ Sci Pollut R 1-10. https://doi.org/10.1007/s11356-017-1103-
651 y
652 Kataki S, Hazarika S, Baruah DC (2017) Investigation on by-products of bioenergy
653 systems (anaerobic digestion and gasification) as potential crop nutrient using FTIR,
654 XRD, SEM analysis and phyto-toxicity test. J Environ Manage 196:201-216.
655 https://doi.org/10.1016/j.jenvman.2017.02.058
656 Kebelmann K, Hornung A, Karsten U, Griffiths G (2013) Intermediate pyrolysis and
657 product identification by TGA and Py-GC/MS of green microalgae and their extracted
658 protein and lipid components. Biomass Bioenerg 49:38-48.
659 https://doi.org/10.1016/j.biombioe.2012.12.006
660 Kim BS, Lee HW, Park SH, Baek K, Jeon JK, Cho HJ, et al. (2016) Removal of Cu^{2+}
661 by biochars derived from green macroalgae. Environ Sci Pollut R 23:985-994.
662 https://doi.org/10.1007/s11356-015-4368-z

663 Li Q, Lu Y, Guo X, Shan G, Huang J (2017) Properties and evolution of dissolved
664 organic matter during co-composting of dairy manure and Chinese herbal residues.
665 Environ Sci Pollut R 24:8629-8636. https://doi.org/10.1007/s11356-017-8540-5
666 Liu F, Rotaru AE, Shrestha PM, Malvankar NS, Nevin KP, Lovley DR (2012)
667 Promoting direct interspecies electron transfer with activated carbon. Energ Environ Sci
668 5:8982-8989. 10.1039/C2EE22459C
669 Liu X, He R, Shi Y, Yan Z, Wang C, Jiang H (2016) Identifying the Chemical
670 Composition of Decomposed Residues From Cyanobacterial Bloom Biomass by
671 Pyrolysis-GC/MS. CLEAN–Soil Air Water 44:1636-1643. 10.1002/clen.201500283
672 Lovley DR (2017) Happy together: microbial communities that hook up to swap
673 electrons. ISME J 11:327-336. doi:10.1038/ismej.2016.136
674 Luo C, Lü F, Shao L, He P (2015) Application of eco-compatible biochar in anaerobic
675 digestion to relieve acid stress and promote the selective colonization of functional
676 microbes. Water Res 68:710-718. https://doi.org/10.1016/j.watres.2014.10.052
677 Martínez EJ, Gil MV, Fernandez C, Rosas JG, Gómez X (2016) Anaerobic codigestion
678 of sludge: addition of butcher's fat waste as a cosubstrate for increasing biogas
679 production. PloS one, 11:e0153139. https://doi.org/10.1371/journal.pone.0153139
680 Martínez EJ, Gil MV, Rosas JG, Moreno R, Mateos R, Morán A, Gómez X (2017)
681 Application of thermal analysis for evaluating the digestion of microwave pre-treated
682 sewage sludge. J Ther Anal Calorim 127:1209-1219. https://doi.org/10.1007/s10973-
683 016-5460-4
684 Moestedt J, Müller B, Westerholm M, Schnürer A (2016) Ammonia threshold for
685 inhibition of anaerobic digestion of thin stillage and the importance of organic loading
686 rate. Microb Biotechnol 9:180-194. 10.1111/1751-7915.12330

687 Mopper K, Stubbins A, Ritchie JD, Bialk HM, Hatcher PG (2007) Advanced
688 instrumental approaches for characterization of marine dissolved organic matter:
689 extraction techniques, mass spectrometry, and nuclear magnetic resonance
690 spectroscopy. Chem Rev 107:419-442. 10.1021/cr050359b
691 Palatsi J, Affes R, Fernandez B, Pereira MA, Alves MM, Flotats X (2012) Influence of
692 adsorption and anaerobic granular sludge characteristics on long chain fatty acids
693 inhibition process. Water Res 46:5268-5278.
694 https://doi.org/10.1016/j.watres.2012.07.008
695 Prasad S, Schmidt H, Lampen P, Wang M, Güth R, Rao JV, Eiceman GA (2006)
696 Analysis of bacterial strains with pyrolysis-gas chromatography/differential mobility
697 spectrometry. Analyst 131:1216-1225. 10.1039/B608127D
698 Provenzano MR, Carella V, Malerba AD (2015) Composting Posidonia oceanica and
699 sewage sludge: Chemical and spectroscopic investigation. Compost Sci Util 23:154-
700 163. https://doi.org/10.1080/1065657X.2015.1013586
701 Roth S, Spiess AC (2015) Laccases for biorefinery applications: a critical review on
702 challenges and perspectives. Bioproc Biosyst Eng 38:2285-2313.
703 https://doi.org/10.1007/s00449-015-1475-7
704 Song XD, Chen DZ, Zhang J, Dai XH, Qi YY (2017) Anaerobic digestion combined
705 pyrolysis for paper mill sludge disposal and its influence on char characteristics. J Mater
706 Cycles Waste 19: 332-341. https://doi.org/10.1007/s10163-015-0428-1
707 Tyagi VK, Lo SL, Rajpal A (2014) Chemically coupled microwave and ultrasonic pre-
708 hydrolysis of pulp and paper mill waste-activated sludge: effect on sludge solubilisation
709 and anaerobic digestion. Environ Sci Pollut R 21:6205-6217.
710 https://doi.org/10.1007/s11356-013-2426-y

711 Volkman JK (1986) A review of sterol markers for marine and terrigenous organic
712 matter. Organic Geochem 9:83-99. https://doi.org/10.1016/0146-6380(86)90089-6
713 Wang C, Anderson C, Suárez-Abelenda M, Wang T, Camps-Arbestain M, Ahmad R,
714 Herath HMSK (2015) The chemical composition of native organic matter influences the
715 response of bacterial community to input of biochar and fresh plant material. Plant Soil
716 395:87-104. https://doi.org/10.1007/s11104-015-2621-3
717 Wang K, He C, You S, Liu W, Wang W, Zhang R, Ren N (2015) Transformation of
718 organic matters in animal wastes during composting. J Hazard Mater 300:745-753.
719 https://doi.org/10.1016/j.jhazmat.2015.08.016
720 Wang T, Qin Y, Cao Y, Han B, Ren J (2017) Simultaneous addition of zero-valent iron
721 and activated carbon on enhanced mesophilic anaerobic digestion of waste-activated
722 sludge. Environ Sci Pollut R 24:22371-22381. https://doi.org/10.1007/s11356-017-
723 9859-7
724 Wilson MA, Gillam AH, Collin PJ (1983) Analysis of the structure of dissolved marine
725 humic substances and their phytoplanktonic precursors using 1H and 13CNMR. Chem
726 Geol 40:187-201. https://doi.org/10.1016/0009-2541(83)90029-3
727 Wu S, Lou R, Lv G (2010) Analysis of wheat straw lignin by thermogravimetry and
728 pyrolysis–gas chromatography/mass spectrometry. J Anal Appl Pyrol 87:65-69.
729 https://doi.org/10.1016/j.jaap.2009.10.006
730 Yeneneh AM, Sen TK, Ang HM, Kayaalp A (2017) Optimisation of microwave,
731 ultrasonic and combined microwave-ultrasonic pre-treatment conditions for enhanced
732 anaerobic digestion. Water Air Soil Poll 228:11. https://doi.org/10.1007/s11270-016-
733 3197-0

734 Zhao J, Peng P-A, Song J, Ma S, Sheng G, Fu J, Yuan D (2012) Characterization of
735 humic acid-like substances extracted from atmospheric falling dust using Py-GC-MS.
736 Aerosol Air Qual Res 12:83-92. doi: 10.4209/aaqr.2011.06.0086
737 Zhu R, Versteegh GJ, Hinrichs KU (2016) Detection of microbial biomass in
738 subseafloor sediment by pyrolysis–GC/MS. J Anal Appl Pyrol 118:175-180.
739 https://doi.org/10.1016/j.jaap.2016.02.002
740

741

742 Figure caption

743

744 **Fig. 1** (a) Specific methane production of SM and (b) ammonium content obtained from
745 batch digestion tests. (c) VFA results obtained from the digestion of SM, (d) pre-treated
746 SM (SM_MW), (e) SM supplemented with char (SM_Char), and (f) and pre-treated SM
747 supplemented with char (SM_MW_Char)

748

749 **Fig. 2** Results from scanning electron microscopy. Surface of char, digestate and
750 digestate containing char particles. Samples were obtained from batch digestion
751 experiments

752

753 **Fig. 3** FTIR spectra of the initial and digestate samples obtained from the batch
754 digestion of swine manure (SM), the pre-treated SM (SM_MW) and systems
755 comprising the addition of Char (SM_Char and SM_MW_Char)

756

757 **Fig. 4** (a) Chromatograms of pyrolysis products released from substrate samples,
758 inoculum and digestates obtained at the end of the experiment. Statistical analysis: (b)
759 HCA and (c) PCA

760

761

762

763 Table 1. Chemical characteristics of inoculum and swine manure (SM).

764

765 Table 2. Results from proximate and ultimate analysis of initial samples and digestates.

766

767 Table 3. Results obtained from batch digestion test of swine manure (SM), pre-treated

768 SM (SM_MW) and char supplemented systems (SM_Char, SM_MW_Char).

769

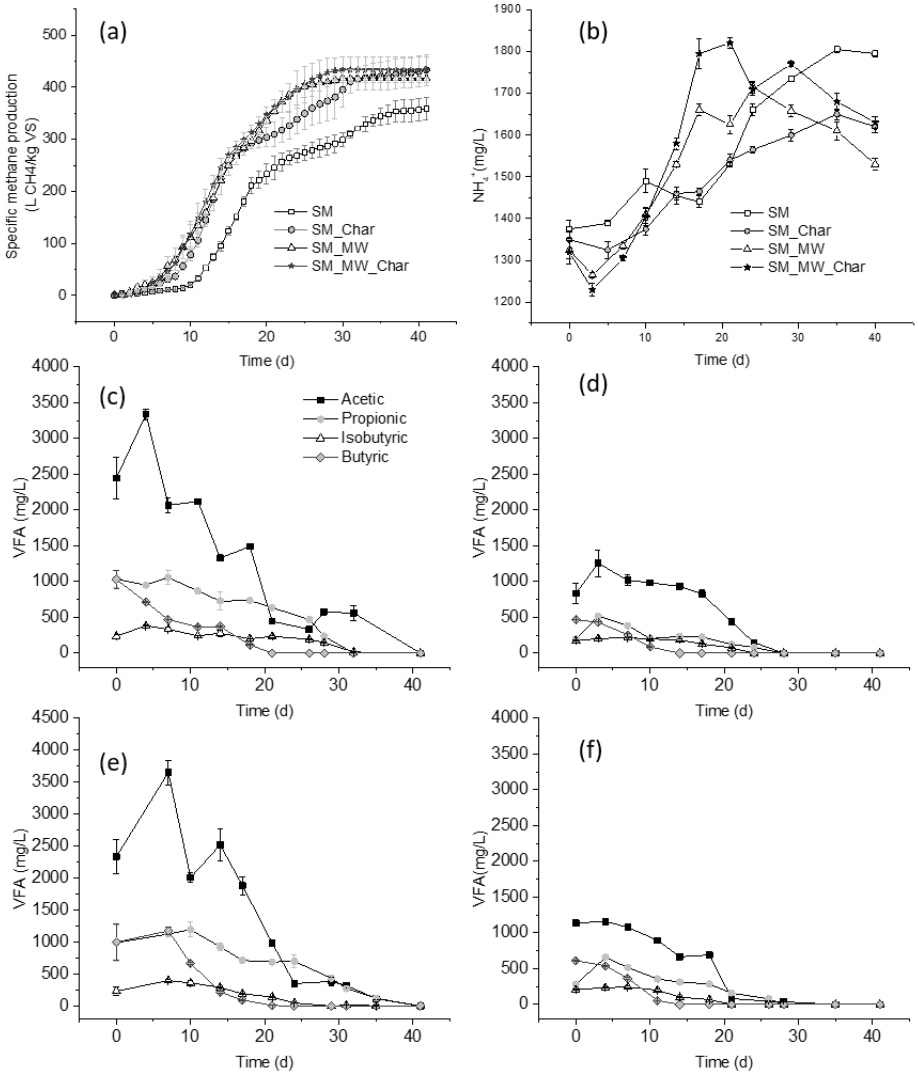
(a)
Specific methane production (L CH4/kg VS)
SM
SM_Char
SM_MW
SM_MW_Char
Time (d)
(b)
NH4+ (mg/L)
SM
SM_Char
SM_MW
SM_MW_Char
Time (d)
(c)
Acetic
Propionic
Isobutyric
Butyric
VFA (mg/L)
Time (d)
(d)
VFA (mg/L)
Time (d)
(e)
VFA (mg/L)
Time (d)
(f)
VFA(mg/L)
Time (d)

770

771

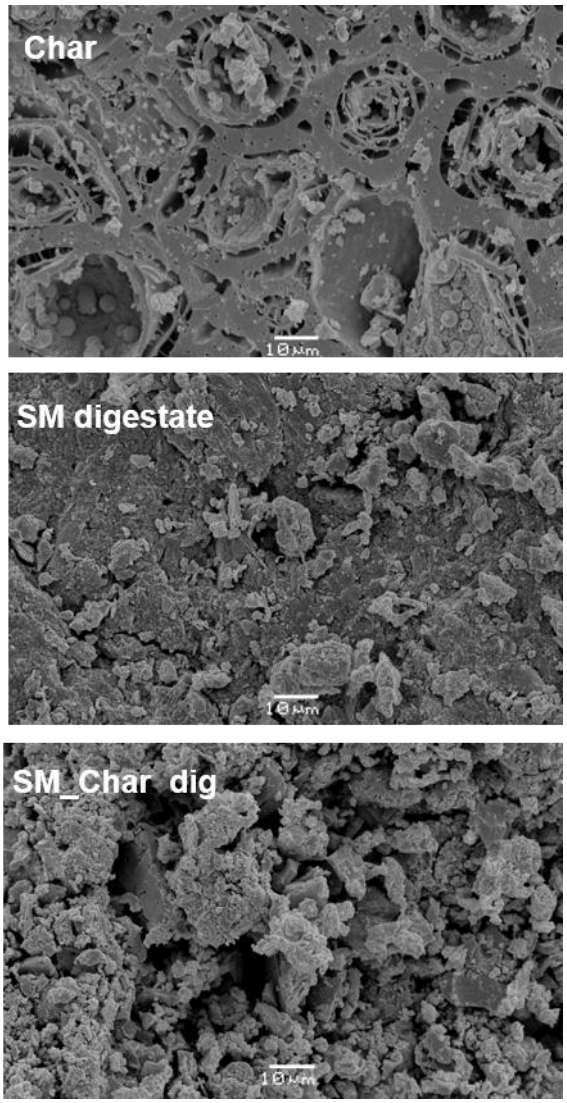

772

773

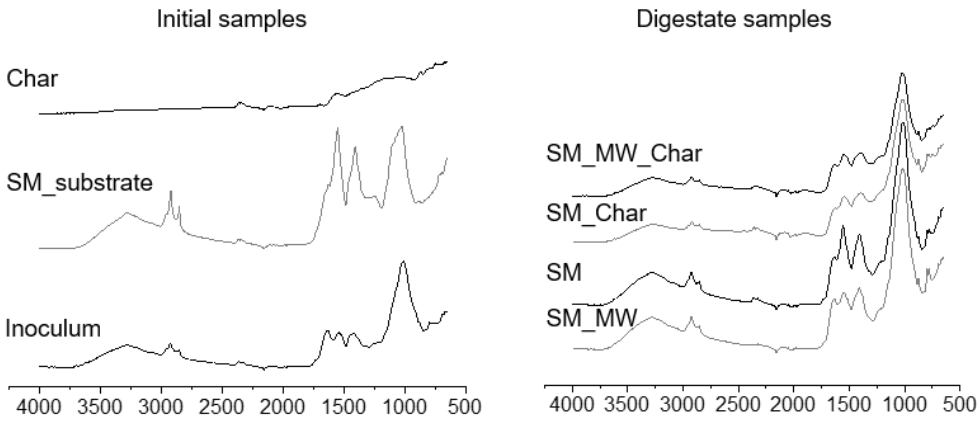
Initial samples
Digestate samples
Char
SM_substrate
Inoculum
SM_MW_Char
SM_Char
SM
SM_MW
4000 3500 3000 2500 2000 1500 1000 500
4000 3500 3000 2500 2000 1500 1000 500

774

775

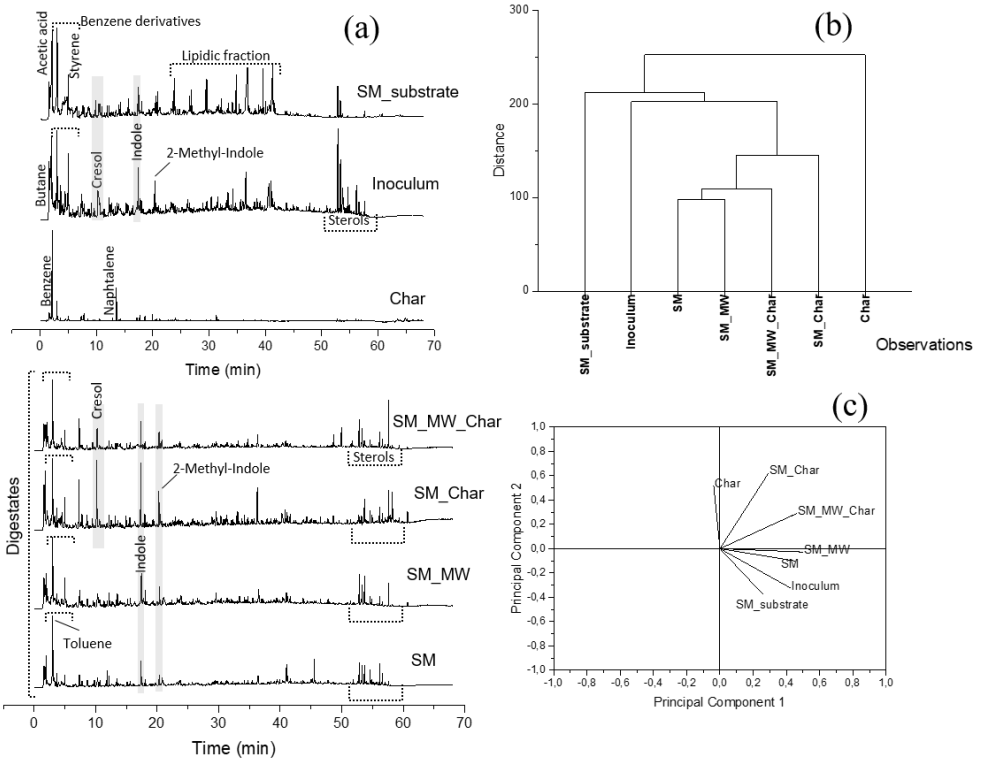
(a)
Acetic acid
Benzene derivatives
Styrene
Lipidic fraction
SM_substrate
Butane
Cresol
Indole
2-Methyl-Indole
Inoculum
Sterols
Benzene
Naphtalene
Char
Time (min)
Digestates
Cresol
SM_MW_Char
Sterols
2-Methyl-Indole
SM_Char
Indole
SM_MW
Toluene
SM
Time (min)
(b)
Distance
SM_substrate
Inoculum
SM
SM_MW
SM_MW_Char
SM_Char
Char
Observations
(c)
Principal Component 2
Principal Component 1
Char
SM_Char
SM_MW_Char
SM_MW
SM
Inoculum
SM_substrate

776

777

Table 1. Chemical characteristics of inoculum and swine manure (SM).

Feedstock	TS (g/L)	VS (g/L)	TN (g/kg) [a]	P (ppm) [a]	pH	C/N	NH_4^+ (mg/L)
SM	23.1	15.2	3.6	12 207	6.9	10.9	3 085
Inoculum	47.6	27.8	4.2	22 452	7.5	8.5	1 050

[a] expressed on a dry basis. TS: Total solids. VS: Volatile solids. TN: Total Kjeldahl nitrogen.

784 Table 2. Results from proximate and ultimate analysis of initial samples and digestates.
785

Sample	Proximate analysis			Ultimate analysis				
	Moisture (%)	Volatiles (%)	Ash (%)	C (%)	H (%)	N (%)	S (%)	O (%)
SM_substrate	8.6	61.1	27.2	40.1	4.8	4.3	1.24	49.6
Inoculum	4.8	49.9	40.9	32.0	4.2	4.2	1.5	58.0
Char	3.9	8.9	3.1	90.4	2.1	0.4	0.1	7.1
Digestates								
SM	5.2	44.6	46.7	28.9	3.6	3.2	1.4	63.0
SM_Char	5.3	31.7	28.8	52.8	2.9	2.2	0.9	41.2
SM_MW	5.2	44.0	46.1	28.1	3.4	2.8	1.6	64.1
SM_MW_Char	5.0	30.9	28.1	53.9	2.9	2.1	1.0	40.1

786
787

788 Table 3. Results obtained from batch digestion test of swine manure (SM), pre-treated
789 SM (SM_MW) and char supplemented systems (SM_Char, SM_MW_Char).
790

Parameter	SM	SM_Char	SM_MW	SM_MW_Char
Cumulative CH_4 production (mL)	448.1 ± 19.7	593.1 ± 50.4	625.5 ± 4.1	649.8 ± 36.9
CH_4 Yield (mL/g VS)	298.7 ± 23.8	395.4 ± 42.7	416.7 ± 27.9	433.2 ± 37.9
CH_4 (%)	68.9 ± 1.7	69.3 ± 1.7	73.3 ± 1.6	75.3 ± 1.7
$pH_{initial}$	7.0 ± 0.1	7.1 ± 0.1	7.7 ± 0.1	7.9 ± 0.1
pH_{final}	8.0 ± 0.1	8.0 ± 0.1	7.8 ± 0.1	8.1 ± 0.1
Modified Gompertz model parameters				
λ (d)	9.19 ± 0.21	6.07 ± 0.22	5.88 ± 0.09	5.83 ± 0.07
Pmax (mL/kg VS)	349.6 ± 5.1	426.1 ± 6.0	428.8 ± 2.4	441.2 ± 1.9
Rmax (mL/kg VS d)	21.2 ± 3.9	24.5 ± 4.5	27.5 ± 2.3	28.8 ± 1.8
R^2	0.992	0.990	0.998	0.999

791
792

Fig. SM1. Chromatograms of pyrolysis products released from substrate samples, inoculum and char

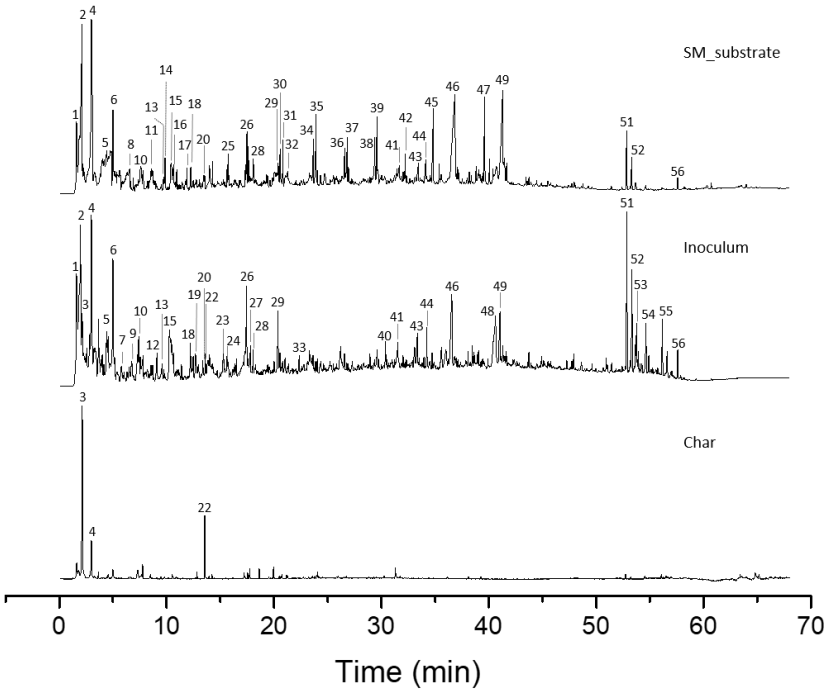

793
794

Fig. SM2. Chromatograms of pyrolysis products released from digested samples

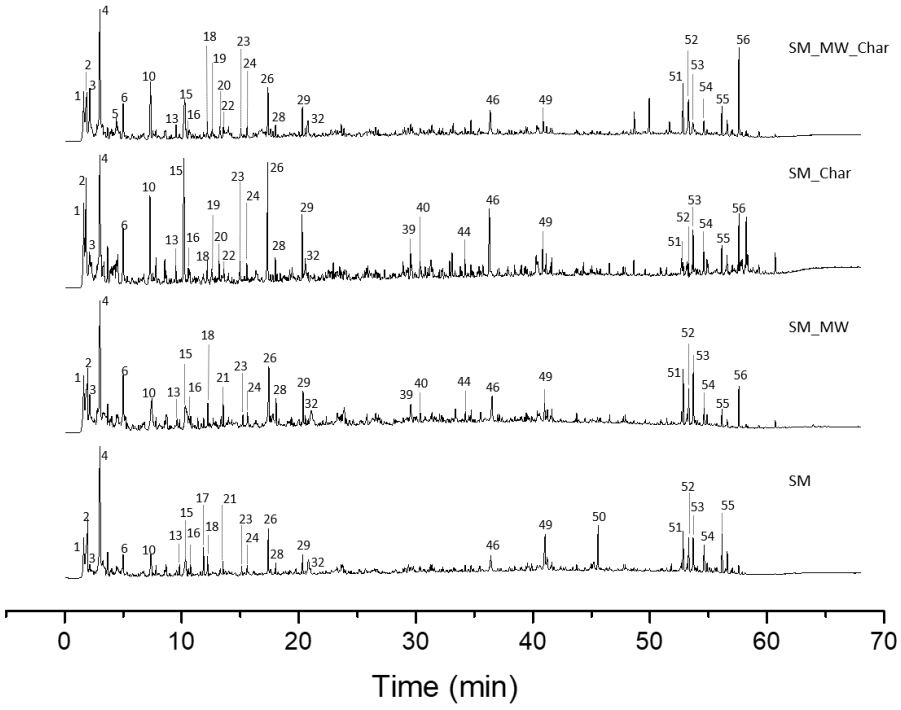

795

796

797 Table SM1. Selected pyrolysis fragments identified from substrates and digested
798 samples.
799

No	Compound	m/z
1	Butane	43, 58
2	Acetic acid	43, 60
3	Benzene	78
4	Toluene	91, 92
5	C2-benzene	91, 106
6	Styrene	78, 104
7	Furfural	95, 96
8	Pentanoic acid	60, 73
9	5-Methyl furfural	109, 110
10	Phenol	66, 94
11	2-Propenyl Benzene	91, 103, 117
12	Indene	115, 116
13	o-Cresol, m-Cresol	107, 108
14	acetophenone	77, 105, 120
15	p-Cresol	107, 108
16	2-Methoxy-phenol (guaiacol)	109, 124
17	Benzyl methyl ketone	43, 91, 134
18	Benzeneacetonitrile	90, 117
19	2,5-Dimethyl phenol	107, 122
20	2-Ethyl-phenol, 4-Ethyl-phenol	107, 122
21	Methyl-phenyl-acetate	91, 150
22	Naphtalene	128
23	Coumaran	91, 120
24	Benzenepropane nitrile	91, 131
25	2-Butanone-4-phenyl	91, 105, 148
26	Indole	90, 117
27	Methyl-naphtalene	115, 142
28	Vinylguaiacol	135, 150
29	2-Methyl-indole	130, 131
30	Tetradecene	41, 43, 55, 70, 83, 97
31	Tetradecane	43, 57, 71, 85
32	Ethylguaiacol	137
33	Eugenol	149, 164
34	1-Pentadecene	55, 69, 83
35	Pentadecane	57, 71, 85
36	1-Hexadecene	55, 69, 83
37	Hexadecane	57, 71, 85
38	1-Hexadecanol, 2-methyl	57, 69, 83, 97
39	Tedradecane, 2, 6, 10-trimethyl	57, 71, 85
40	1-Dodecanol 3,7,11-trimethyl	57, 69, 83, 97, 111
41	Tetradecanoic acid	60, 73, 129, 185
42	Phytol	57, 71, 81
43	i-Propyl 12-methyltetradecanoate	
44	Pentadecanoic acid	60, 73, 85, 97
45	2-Heptadecanone	58, 71
46	Hexadecanoic acid	60, 73, 83, 129

47	2-Nonadecanone	58, 71
48	6-Octadecenoic acid	55, 69, 83, 97, 11
49	Octadecanoic acid	60, 73, 129
50	Octadecanamide	59, 72
51	Cholest-3-ene,(5β)-	135, 147
52	Cholest-2-ene	147, 161
53	Squalene	69,81
54	Cholesta-3,5-diene	147, 159
55	Methyl 3-hydroxycholestan-26-oate	
56	Coprostanol	135, 149, 161